ELSEVIER

Biochimica et Biophysica Acta 1508 (2000) 69–85

BIOCHIMICA ET BIOPHYSICA ACTA
BBA

www.elsevier.com/locate/bba

Review

Titration calorimetry of surfactant–membrane partitioning and membrane solubilization

H. Heerklotz, J. Seelig *

Department of Biophysical Chemistry, Biocenter of the University of Basel, Klingelbergstrasse 70, CH-4056 Basel, Switzerland

Abstract

The interaction of surfactants with membranes has been difficult to monitor since most detergents are small organic molecules without spectroscopic markers. The development of high sensitivity isothermal titration calorimetry (ITC) has changed this situation distinctly. The insertion of a detergent into the bilayer membrane is generally accompanied by a consumption or release of heat which can be measured fast and reliably with modern titration calorimeters. It is possible to determine the full set of thermodynamic parameters, i.e., the partitioning enthalpy, the partitioning isotherm, the partition coefficient, the free energy, and the entropy of transfer. The application of ITC to the following problems is described: (i) measurement of the critical micellar concentration (CMC) of pure detergent solutions; (ii) analysis of surfactant-membrane partitioning equilibria, including asymmetric insertion; and (iii) membrane-surfactant phase diagrams. Finally, the thermodynamic parameters derived for non-ionic detergents are discussed and the affinity for micelle formation is compared with membrane incorporation.

Keywords: Isothermal titration calorimetry; ITC; Partition coefficient; Membrane solubilization; Flip-flop; Enthalpy; Critical micelle concentration; Lipid–detergent interaction

1. Isothermal titration calorimetry: a short description of the technique

Isothermal titration calorimetry (ITC) measures the heats associated with the mixing and the reaction of two solutions of different compositions. Both physical (non-covalent binding) and chemical processes may be accompanied by a release or uptake of heat. The schematic diagram of a titration calorimeter is shown in Fig. 1. It contains a reference cell and a measuring cell (both with a cell volume of $\sim$1 ml) filled with the same solution. In the measuring cell the reactant is injected via a syringe driven by a stepping motor. The tip of the syringe is flat and acts as a stirrer since the syringe is rotating with a speed of about 300 rpm. The reactant is injected in small aliquots of typically 5–20 μl and the heat produced or consumed is measured as a function of time. The calorimeter is an adiabatic calorimeter working in a power compensation mode [1]. Power compensation means that all heats effects arising from the injection are actively balanced by the calorimeter feedback keeping the reference cell and the measuring cell at the same temperature. This is realized in practice by a very precise measurement of the temperature difference between the two cells. The reference cell is heated continuously with a very low power ('RO') of e.g., 20 μW. Because the increase in temperature

* Corresponding author. Fax: +41-61-267-2189;
E-mail: joachim.seelig@unibas.ch

0005-2736/00/$ – see front matter
PII: S0304-4157(00)00009-5

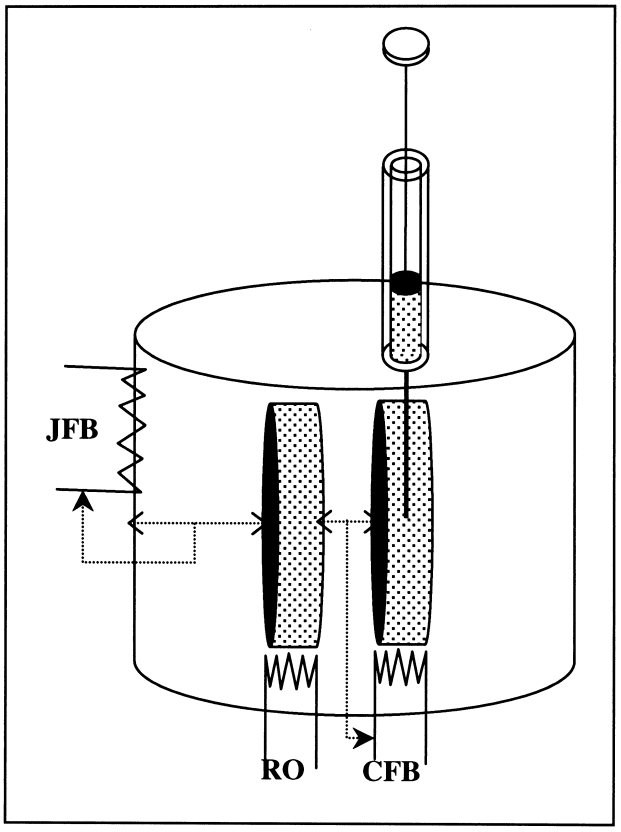

Fig. 1. Schematic diagram of a titration calorimeter (cf. text).

is also low (30–60 mK/h), the mixing and reaction process can be considered as 'isothermal' within the limits of the experiment. The mixing cell is connected to a second heater ('CFB'), the power of which is controlled by a feedback mechanism eliminating any temperature differences between reference cell and measuring cell. The 'baseline value' of the CFB will be similar to that of the reference cell because size and content of the two cells are matched. If heat is produced or consumed in the measuring cell upon injection of a reactant, a change in the CFB power is required to restore identical temperatures in the two cells. The heat flow is measured and recorded as a function of time. The integration of the CFB heat flow yields the heat of reaction.

Reference and mixing cell are shielded from the environment by an adiabatic jacket which is heated by a third heating system ('JFB') keeping the temperature of the adiabatic shield exactly at that of the reference cell. In the absence of a temperature gradient no heat exchange can occur with the environment.

Isothermal titration calorimetry (ITC) has a number of advantages. Almost all chemical and physical processes entail heat changes and can thus be measured with ITC without the need for a specific spectroscopic or isotopic labeling. The instrument is highly sensitive and measures heats of reaction of $\sim$1 μcal (10^{-6} K temperature change for a 1 ml cell), and it is thus possible to measure small amounts of dilute reactants. Moreover, the measurement is fast and a single titration sequence with 20 injections is usually finished within 90 min. Finally, it is possible to derive the complete thermodynamic picture of the physical or chemical process under consideration, i.e., the enthalpy, ΔH, the free energy, ΔG, and the entropy, ΔS.

ITC has proven extremely useful to study *surfactant–membrane equilibria* and four types of experiment can broadly be distinguished:

- measurement of the critical *micellar concentration* (CMC);
- the *partition equilibrium* between monomeric surfactant and the lipid membrane;
- *membrane solubilization* at high concentrations of surfactant; and
- *membrane formation* upon dilution of mixed lipid–surfactant micelles.

ITC measurements provide the relevant concentrations such as the CMC and the critical concentrations for the onset and end of membrane solubilization, as well as the partition constant and the reaction enthalpy. ITC can also be used to establish a partial *phase diagram* of surfactant–lipid mixtures.

2. Critical micellar concentration

ITC is a convenient tool to determine the critical micellar concentration (CMC) and the heat of micelle formation, $\Delta H_{mic} = \Delta H_D^{w\rightarrow m}$. The second notation specifies that ΔH_{mic} is the molar enthalpy of transfer of detergent (D) monomers from water (w) into micellar (m) aggregates. Experimentally, the CMC is determined by studying *demicellization*, i.e., the reverse process of micelle formation [2–8]. A sur-

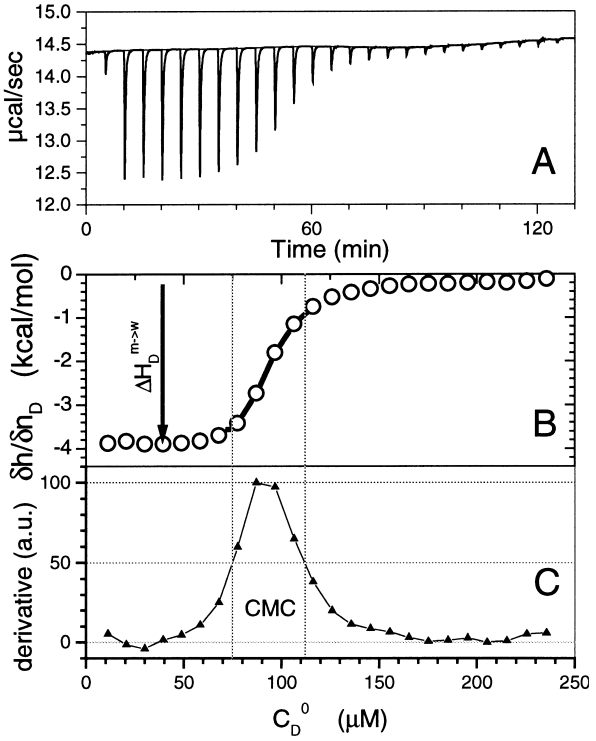

Fig. 2. Determination of the critical micellar concentration (CMC). A 2.5 mM solution of $C_{12}EO_8$ in water is injected into pure water. (A) Heat flow (the power of the CFB heater) vs. time. (B) Integrated heat per injection, δh_i, normalized with respect to the injected number of moles, δn_D^0. Initially, micelles are completely dissolved and the heat of demicellization is $\Delta H_D^{m\rightarrow w} = -3.6$ kcal/mol. As the surfactant concentration increases, the process of demicellization comes to a halt and the reaction enthalpy approaches zero (with a small heat of dilution remaining). The CMC is defined as the midpoint of the sigmoidal transition curve and is CMC = 90 ± 20 µM. (C) Midpoint and width of the micelle→monomer transition are defined more clearly by calculating the first derivative of the transition curve B.

factant solution with a concentration well above the CMC ($C_D^0 >$ CMC) is filled into the syringe and is injected into the measuring cell containing pure water (or buffer). The volume of the measuring cell is $V_{cell} \sim 1$ ml and a 10 µl injection thus leads to a 100-fold dilution of the injected surfactant solution. The micelles dissolve into monomers, a process accompanied by a release or uptake of heat. This is demonstrated in Fig. 2 for the demicellization of $C_{12}EO_8$. The upper panel shows the heat flow caused by the injection of 5 µl aliquots of a 2.5 mM micellar detergent solution into buffer. The heat of each injection, δh_i, is determined by integration of the heat flow peak after subtraction of the baseline. Ignoring the first injection (cf. below), each of the following seven injections causes an exothermic heat of demicellization of about −48 µcal and increases the detergent concentration in the cell in steps of $\delta C_D^0 \approx 9$ µM. The injection heats are divided by the injected mole number (12.5 nmol) of detergent, yielding $\Delta H_D^{m\rightarrow w}$ which is plotted versus C_D^0 (middle panel). The figure illustrates that micelles are dissolved with a molar heat of −3.6 kcal/mol up to the CMC of about (90 ± 20) µM. The reverse process, i.e., micelle *formation*, is endothermic with $\Delta H_D^{w\rightarrow m} = +3.6$ kcal/mol. The CMC is not seen as a sharp 'phase boundary' but is defined as the midpoint of a rather broad transition range. For a more precise quantitation of the midpoint and the width of the micellization process it is advantageous to plot the first derivative of the ΔH vs. C_D^0 curve as shown in the bottom panel.

In general, a number of technical details must be taken into account in analyzing ITC experiments. First, a small heat is measured even for a buffer-into-buffer injection. This is due to temperature differences between the injection syringe and the calorimeter cell. Secondly, changes in the concentration upon consecutive injections lead to heats of dilution which are, however, usually very small. Appropriate control measurements must be performed and must be subtracted. Thirdly, injections into the completely filled calorimeter cell lead to an 'overflow', displacing a corresponding part of the cell content. Again, proper corrections must be applied (cf. below). Finally, the filling and mounting of the syringe may cause a slight inaccuracy of the volume of the first injection. Therefore, a first injection of small volume (2 µl) is often made (Fig. 2A) and the corresponding heat is not included in the evaluation.

The CMCs encompass a wide range of concentrations and Table 1 gives the CMCs of surfactants commonly employed in membrane research. Surfactants with a high CMC are generally preferred in biochemical preparations since they are easily removed by dialysis against buffer.

3. Surfactant partitioning into membranes

If a surfactant is dissolved in the aqueous phase at a concentration distinctly below its critical micellar

Table 1
Micelle formation and partitioning of surfactants into POPC or EYPC membranes at room temperature: thermodynamic parameters[a] (taken from [22])

Surfactant	ΔH^0 (kcal/mol)	K (ITC) (10^3 M^{-1})	CMC (10^{-3} M)	K·CMC
Oligo (ethylene oxide) alkyl ether				
$C_{10}EO_3$	1.9 [22]	6 [22]	0.6 [22]	0.36
$C_{10}EO_7$	6.5 [22]	0.77 [22]	0.85 [22]	0.65
$C_{12}EO_3$	1.3 [22]	100 [22]	0.06 [16,22]	6
$C_{12}EO_4$	2.9 [22]	35 [22]	0.06 [16,22]	2.1
$C_{12}EO_5$	3.8 [22]	24 [22]	0.065 [4,16]	1.56
$C_{12}EO_6$	4.8 [22]	20 [22]	0.065 [4,16]	1.3
$C_{12}EO_7$	4.8 [22]	12 [22]	0.075 [16,22]	0.9
$C_{12}EO_8$	7.7 [22]	6 [22]	0.09 [4,7]	0.54
Tritons				
X-100	3.6 [22]	3.0 [22]	0.23 [17,22]	0.69
X-114	1.9 [22]	3.5 [22]	0.17 [43]	0.59
Alkyl (thio) glucosides				
C_8 Gluc	1.3 [21]	0.12 [21]	23 [6,35]	2.3
C_8 Thiogluc	1–2 [18]	0.24 [18]	9 [44,45]	2.1
C_{10} Gluc	1.2 [21]	1.6 [21]	2.2[b] [46]	3.5
Alkyl maltosides				
C_8 Malt	2.4 [22]	0.025 [22]	19.5 [46]	0.49
C_{10} Malt	3.1 [22]	0.2 [22]	1.8 [46]	0.36
C_{12} Malt	1.0 [22]	5 [22]	0.17 [46]	0.85
Phospholipid				
D7PC	1.7 [22]	0.2 [22]	1.9 [22]	0.38
Steroid				
CHAPS	6.9 [22]	0.6 [22]	10 [22]	6

[a]The values of K measured at different detergent concentrations vary by 4–20%, indicating the experimental error and also possible variation of K with the detergent concentration.
[b]Critical aggregation concentration to lamellar structures.

concentration ($C_D^0 \ll$ CMC), it will partition into the membrane without disrupting it. The physical properties of the membrane will gradually change as the surfactant accumulates and the thermodynamic properties may also change with the membrane composition. In the following we shall discuss (i) relevant models to quantitatively describe the partition equilibrium of a surfactant between the aqueous phase and the membrane (called, for short, 'membrane partitioning') and (ii) the calorimetric analysis of the partitioning equilibrium.

3.1. Partitioning models

Let us consider a surfactant–membrane partition equilibrium such that $n_{D,b}$ moles of surfactant are incorporated into the membrane, $n_{D,f}$ moles are in the aqueous phase, and $n_D^0 = n_{D,b} + n_{D,f}$ is the total amount of surfactant. If the membrane is made up of n_L^0 moles of lipid, $R_b = n_{D,b}/n_L^0$ is the molar ratio of membrane-inserted ('bound') detergent to total lipid. The concentration of surfactant in the aqueous phase of volume V is $C_{D,f} = n_{D,f}/V$.

The *mole-ratio partition coefficient* K used by Schurtenberger [9] describes a linear relation between the concentration of surfactant free in solution, $C_{D,f}$, and the surfactant-to-lipid ratio R_b:

$$R_b = KC_{D,f} \quad (1)$$

The partition constant K has the dimension of a reciprocal concentration. Typically, water is much in excess over lipid. If $n_{D,b}$ and n_L^0 are referred to the

total volume V of the aqueous phase with $C_{D,b} = n_{D,b}/V$ and $C_L^0 = n_L^0/V$, Eq. 1 can be rewritten as

$$\frac{C_{D,b}}{C_L^0} = KC_{D,f} \quad (2)$$

Taking into account mass conservation ($C_D^0 = C_{D,b} + C_{D,f}$), a third way to describe this equilibrium is

$$C_{D,b} = C_D^0 \frac{KC_L^0}{1 + KC_L^0} \quad (3)$$

Note that almost complete incorporation of the surfactant into the membrane is realized if $K\,C_L^0 \gg 1$.

The *mole fraction partition coefficient* P [10] is based on the assumption of ideal mixing of surfactant and lipid in the membrane, implying:

$$X_b = PX_f \quad (4)$$

where $X_b = n_{D,b}/(n_{D,b} + n_L^0)$ and $X_f = n_{D,f}/(n_{D,f} + n_w)$ are the mole fractions of surfactant in the lipid and the water phase, respectively. For dilute surfactant solutions, water is much in excess over surfactant, i.e., $n_w \gg n_{D,f}$. If all compounds participating in the equilibrium are furthermore referred to the same volume V, Eq. 4 can be stated as

$$X_b = PC_{D,f}/C_w \quad (5)$$

where $C_w = 55.5$ M is the molar concentration of water. The partition coefficient, P, as defined by Eq. 4 or 5 is dimensionless. Some authors omit the constant factor C_W [11,12] so that the partition coefficient is given in M^{-1}.

The partition constants of the two models, K and P, are related to each other via

$$K = \frac{P}{C_W}\left(1 + \frac{C_{D,b}}{C_L^0}\right) = \frac{P}{C_W}(1 + R_b) \quad (6)$$

If P is constant, K will vary with the membrane composition and vice versa. At low detergent concentrations in the membrane ($R_b \ll 1$), the two models differ only by the constant factor $C_W = 55.5$ M.

Most systems studied so far differ markedly from ideal mixing so that a constant P according to Eq. 4 fails to describe the partitioning adequately. This fact has been explained qualitatively [13] and quantitatively [7,14,15] in terms of statistically abundant, unfavorable detergent/detergent interactions. The subsequent variation of the partition coefficient is described in terms of the non-ideality parameter ρ^0 according to:

$$P(X_b) = P(0)\cdot\exp\left\{-\frac{\rho^0}{RT}\cdot(1-X_b)^2 - 1\right\} = P(1)\cdot\exp\left\{-\frac{\rho^0}{RT}\cdot(1-X_b)^2\right\} \quad (7)$$

$P(0)$ is the partition coefficient for the pure lipid membrane with almost no surfactant, $P(1)$ describes the hypothetical situation of a pure detergent membrane.

Eq. 7 leads to a two-parameter fit of the experimental data whereas Eq. 1 and 4 allow the adjustment of a single parameter only. A schematic comparison of the three models, i.e., Eq. 3, Eq. 4, and the combination of Eq. 4 with Eq. 7 is given in Fig. 3. The *mole fraction* of bound detergent, X_b, and the *detergent-to-lipid ratio*, R_b, are plotted as functions of the free detergent concentration, $C_{D,f}$. The parameters ($K = 1000$ M^{-1}; $P = K\cdot C_W = 55.5\times 10^3$) were chosen such as to yield identical binding isotherms at low surfactant concentrations. The interaction parameter $\rho^0 = -0.4$ kcal/mol was taken from experimental measurements with $C_{12}EO_n$ ($n = 3...8$) and octyl glucoside [14,16]. In Fig. 3A, the mole fraction X_b is shown as a function of $C_{D,f}$. Eq. 4 predicts a straight line while the two other models yield curved binding isotherms with lower X_b values. Fig. 3B represents exactly the same data in the form of a R_b vs. $C_{D,f}$ plot. In this representation Eq. 1 yields the straight line. The most conspicuous result of Fig. 3 is the almost perfect coincidence between the $R_b = K\,C_{D,f}$ and the $X_b = P(X_b)\,C_{D,f}$ model. The term $(1+R_b)$ which transforms P into K (cf. Eq. 5) is a very good approximation for the exponential term in Eq. 7 with $\rho^0 = -0.4$ kcal/mol which is based on theory and validated experimentally. Thus, the physically most realistic of the three models degenerates fortuitously into Eq. 1.

Experimentally it is indeed found that the approximation $K \approx$ const. is a much better approximation than $P \approx$ const. for a large number of non-charged lipid–surfactant systems. As an example we select the partitioning of octyl glucoside into bilayers of 1,2-dimyristoyl-*sn*-glycero-3-phosphocholine (DMPC)

which has been investigated with ITC by Blume and co-workers and has been analyzed in terms of Eq. 4 [14]. At 27°C the partition coefficient P was found to decrease from $P=5600$ at $X_b=0$ to $P=2250$ at $X_b=0.6$ (Fig. 8 in [14]). Using Eq. 6 and taking into account that X_b and R_b are related to each other according to

$$X_b = \frac{R_b}{1+R_b} \text{ and } R_b = \frac{X_b}{1-X_b} \quad (8)$$

we calculate $K(X_b=0)=5600/55.5=101\ M^{-1}$ and $K(X_b=0.6)=2250/(55.5(1-0.6))=101\ M^{-1}$. Thus while P varies by a factor of 2.5, the description of the same data in terms of Eq. 1 leads to a constant K over the whole concentration range investigated.

The two partition constants K and P differ in that K 'counts' the bound detergent only in relation to lipid, whereas P 'counts' the detergent in relation to both lipid and bound detergent. If $K=$const. yields a better description of the experimental results than $P=$const., it can be argued that detergent–detergent interactions are weak and that only lipid–detergent interactions have a favorable energy. The model of regular solutions leads to the same qualitative conclusion since $\rho^0=-0.4$ kcal/mol is negative, favoring lipid–detergent interactions over detergent-detergent and lipid–lipid contacts.

The literature on detergent–membrane partition models is quite complex not only because different models are used but also because 'concentrations' are measured in different units. A more comprehensive comparison of models and definitions can be found in Lasch [17]. Finally, not only K or P may vary with the membrane composition but also the partition enthalpy [15,18].

3.2. Surfactant-into-membrane partitioning measured by ITC

In the following we describe the ITC 'bread-and-butter' experiment to quantitatively measure the surfactant partitioning into the lipid membrane. The partition constant, K, and the heat of transfer, $\Delta H_D^{w\to b}$, of a surfactant from the aqueous phase (w) to the bilayer membrane (b) can be determined simultaneously. Fig. 4 shows the titration of $C_{10}EO_7$ with phospholipid vesicles composed of 1-palmitoyl-2-oleoyl-*sn*-glycero-3-phosphocholine (POPC) (data

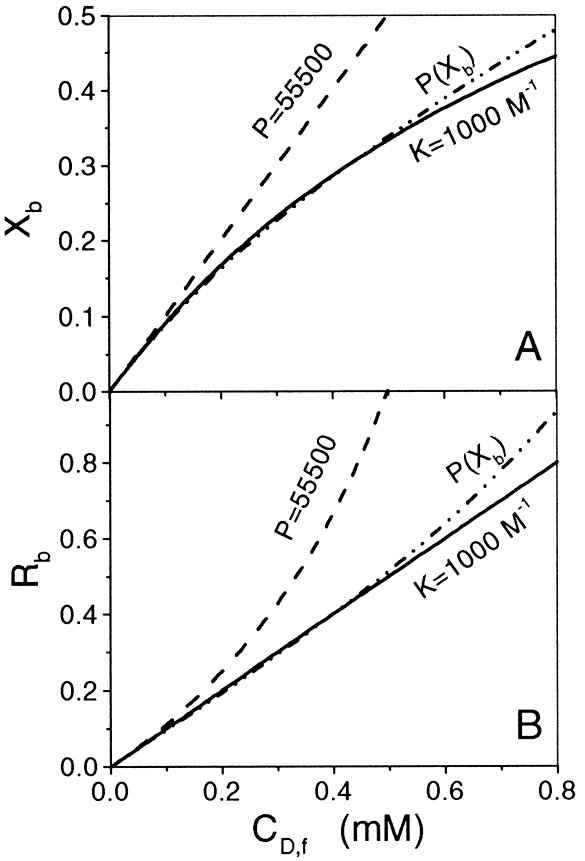

Fig. 3. Comparison of different partition models. The molar detergent-to-lipid ratio in the membrane, $R_b=n_{D,b}/n_L^0$ (A), and the mole fraction, $X_b=n_{D,b}/(n_{D,b}+n_L^0)$ (B) are plotted vs. the concentration of free detergent, $C_{D,f}$. The traces correspond to the partition model (Eq. 1) with $K=1000\ M^{-1}$ (solid lines), the mole fraction model Eq. 4 with $P=C_w\cdot 1000=55'500$ (dashed), and the regular solution model Eq. 7 with $P(0)=55'500$ and $\rho^0=-400$ cal/mol (dash/dot) ($C_w=55.5\ M^{-1}\triangleq$molar concentration of H_2O). All three models merge at very low detergent contents, i.e., R_b, $X_b\to 0$. The regular solution model (Eq. 7) $\rho^0\approx -400$ cal/mol (as measured for a variety of detergents), yields partition isotherms which agree almost perfectly (for not too high R_b values) with the assumption of a constant $K=P(0)/55.5$. In panel A, the mole fraction model $X_b=PC_{D,f}$ yields a straight line and the partition model is curved, in panel B the opposite holds true. In our experience (using isothermal titration calorimetry) most detergents follow the partition model (Eq. 1) at low detergent concentrations.

taken from reference [8]). The phospholipid vesicles have a diameter of ~100 nm, are unilamellar and have been prepared by extrusion. The calorimeter cell contains the surfactant at a concentration $C_D^0=150$ μM which is much below its CMC = 850 μM. The lipid concentration in the injection syringe

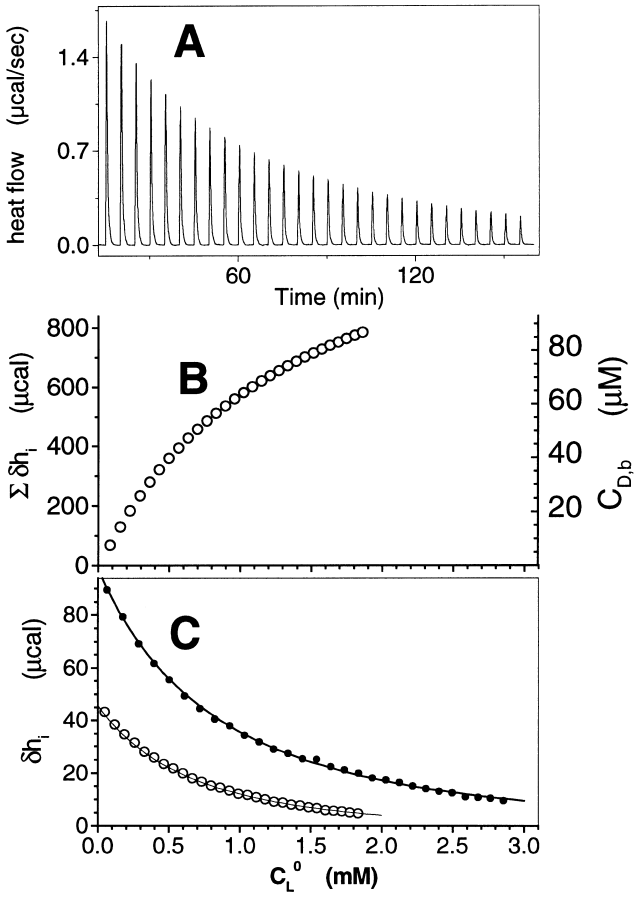

Fig. 4. Titration of $C_{10}E0_7$ with 100 nm POPC vesicles. (A) Calorimetric traces (heat flow) observed upon addition of POPC vesicles ($C_L^0 = 10$ mM) into 150 µM $C_{10}E0_7$, both in buffer (100 mM NaCl, 10 mM Tris, pH 7.4). Ten-µl injections of lipid vesicles at 6-min intervals. (B) Cumulative heats of reaction as obtained from the integration of the calorimetric traces shown in A. The right axis yields the concentration of membrane-bound detergent calculated with Eq. 11 and $\Delta H_D^{w\to b} = 6.5$ kcal/mol. (C) Heats of injection, δh_i, of the data shown in panels A, B (○) and of a second experiment, i.e., 250 µM $C_{10}E0_7$ titrated with 14.8 mM POPC (●). The solid lines correspond to theoretical fits using the partition equilibrium $X_b = K\ C_{D,f}$. The fit parameters were $K = 770\ M^{-1}$ and $\Delta H_D^{w\to b} = 6.5$ kcal/mol.

is $C_L^0 = 10$ mM. Each injection of lipid vesicles leads to partitioning of detergent into the membrane and produces a heat of reaction δh_i (corrected for dilution effects). As the lipid concentration in the calorimeter cell increases, the reaction enthalpies δh_i decrease in magnitude as less and less detergent is available for binding (Fig. 4A). The partition isotherm can be derived from the heats of reaction and can be analyzed in terms of the models discussed above.

This analysis is particularly simple for the partition model Eq. 3. After i lipid injections the molar amount (concentration) of bound surfactant in the calorimeter cell is $n_{D,b}(i)$ ($C_{D,b}(i)$) and the cumulative heat released is

$$\sum_{k=1}^{i} \delta h_k = n_{D,b}^{(i)} \Delta H_D^{w\to b} = \Delta H_D^{w\to b} C_{D,b}^{(i)} V_{cell} \quad (9)$$

$$= \Delta H_D^{w\to b} V_{cell} C_D^0 \frac{K C_L^0}{1 + K C_L^0} \quad (10)$$

where C_D^0 and $C_L^0 = i\delta C_L^0$ are the total detergent and lipid concentration, respectively, in the calorimeter cell after i lipid injections.

Thus it is possible to evaluate K and $\Delta H_D^{w\to b}$ simultaneously by a fit of the measured *cumulative heat* (Fig. 4B) [19–21]. If $\Delta H_D^{w\to b}$ is known, the cumulative heat can be directly converted into the bound amount of detergent using (cf. right axis in Fig. 4B):

$$C_{D,b}^{(i)} = \frac{\sum_{k=1}^{i} \delta h_k}{\Delta H_D^{w\to b}} V_{cell} \quad (11)$$

As an alternative to Eq. 10 it is possible to fit the individual δh_i as a function of C_L^0 [7,14,22]. If the lipid concentration in the measuring cell is increased by steps of δC_L^0, derivation of Eq. 3 predicts a change in the concentration of bound detergent of

$$\delta C_{D,b}^{(i)} = C_D^0 \frac{K}{(1 + K C_L^0)^2} \delta C_L^0 \quad (12)$$

with $C_L^0 = i\ \delta C_L^0$. The corresponding heat of injection is

$$\delta h_i = C_D^0 \Delta H_D^{w\to b} V_{cell} \frac{K}{(1 + iK\delta C_L^0)^2} \delta C_L^0 \quad (13)$$

The simulation of δh_i is shown in Fig. 4C for the experimental results of two different detergent concentrations C_D^0 using the same set of parameters K and $\Delta H_D^{w\to b}$. The fitting of the δh_i values is usually better than fitting of the integrated curve. Integration introduces smoothing of the curves. The curvature of the δh_i plots is more pronounced.

As mentioned above the injection of a lipid sus-

pension leads to a small dilution of the initial detergent concentration in the measuring cell, e.g., 20 injections with $V_{inj} = 10$ μl increase the initial volume of $V_{cell} \sim 1$ ml cell by some 15–20%. With each injection the detergent concentration in the cell decreases by a factor of $V_{cell}/(V_{cell}+V_{inj})$ leading to a total dilution of ($V_{cell} \gg V_{inj}$)

$$C_D^0(i) = C_D^0\left(\frac{V_{cell}}{V_{cell}+V_{inj}}\right)^i \approx C_D^0\frac{V_{cell}}{V_{cell}+iV_{inj}} \qquad (14)$$

Other correction protocols are also conceivable which depend, in part, on the specific operating mode of the calorimeter used. The dilution effect must also be included in the evaluation of the *lipid* concentration.

3.3. Asymmetric membrane insertion of surfactant

In the above examples it was tacitly assumed that *all* lipid C_L^0 would be available for surfactant partitioning. Indeed, most neutral detergents can easily translocate from one halflayer to the other. On the other hand, it is known from isotope labeling experiments that some detergents bind asymmetrically to the membrane, i.e., they insert only into that halflayer which is accessible to them from the respective aqueous phase [23]. At first glance, ITC measurements appear not to be useful to differentiate between the two situations. Inspection of Eqs. 3 or 11–13 reveals that it is the product $K\ C_L^0$ (or $K\ \delta C_L^0$) which determines the shape of the binding isotherm. Any pair (K/γ); ($\gamma\ C_L^0$) is equally well suited to fit the experimental data. If a detergent binds only to the outer monolayer of a sonicated lipid vesicle of 30 nm diameter, 60% of the total lipid is available and the asymmetry parameter is $\gamma = 0.6$. The binding constant increases correspondingly from K to K/γ. For vesicles with larger diameters both halflayers contain an equal number of lipid molecules and the asymmetry parameter is $\gamma = 0.5$.

The mode of binding can however be deduced by combining the binding assay discussed above with a release assay [24]. In the latter, lipid vesicles are prepared in buffer that also contains detergent, leading to a symmetric distribution of detergent molecules in both halves of the membrane. If these vesicles are injected into pure buffer, detergent molecules must be released from the membrane to establish a new equilibrium. However, if the detergent cannot translocate rapidly across the membrane, 40–50% of the vesicle-bound detergent will be entrapped in the inner monolayer and is thus not available for exchange. A comparison of the binding and the release experiment then allows a decision of the two types of models, i.e., either with flip-flop or without flip-flop. Only one of the models leads to a consistent set of parameters K and γ. The evaluation of the partition enthalpy is not influenced by the detergent flip-flop.

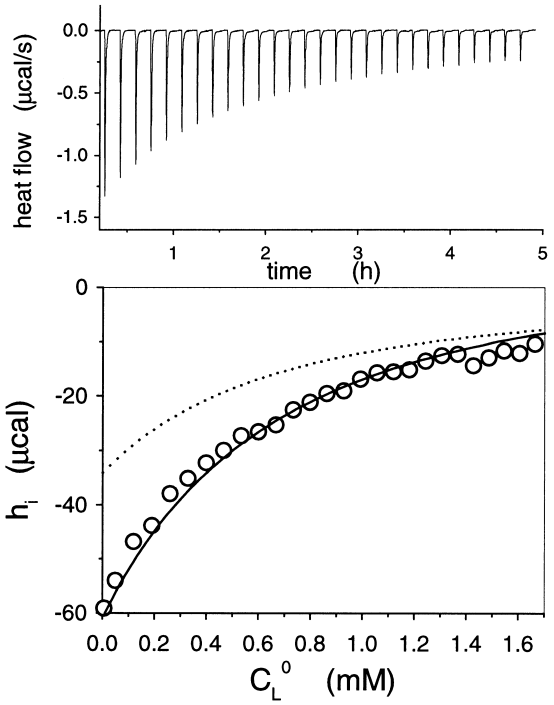

Fig. 5. Detergent release experiment. POPC vesicles ($C_L^0 = 10$ mM, diameter $d = 100$ nm) are prepared by extrusion in a solution of 1 mM $C_{10}EO_7$. The detergent is distributed evenly among the two halves of the bilayer. The mixed lipid–detergent vesicles are filled into the injection syringe. Ten-μl injections into buffer are made. (A) Heat flow h_i. (B) Heat of dilution and detergent release from the membrane. Solid line: theoretical prediction using Eq. 15 with $\gamma = 1$ (i.e., rapid flip-flop), $K = 770$ M^{-1} and $\Delta H_D^{w\to b} = 6.5$ kcal/mol as obtained in Fig. 4. Dotted line: $\gamma = 0.5$ (no flip-flop), other parameters identical.

As an example, Fig. 5 shows this dilution experiment for lipid vesicles composed of 10 mM POPC (1-palmitoyl-2-oleoyl-*sn*-glycero-3-phosphocholine) and 1 mM surfactant ($C_{10}EO_7$) and prepared by extrusion through 100 nm polycarbonate filters. In the starting solution, 98% of the detergent is membrane-bound ($K = 770$ M^{-1}). After a 140-fold dilu-

tion (10 μl injection into 1.4 ml buffer) Eq. 3 predicts that 35% $C_{10}EO_7$ remains membrane-bound, if rapid translocation is assumed, but that 73% remains bound without a flip-flop. The experimental data agree with the rapid flip-flop model.

Subsequent injections lead to smaller heats because less detergent is released with increasing lipid concentration. The analysis of the complete titration curve based on the mole fraction model with a constant P (Eq. 4) has been derived in [24]. However, according to our experience, detergent partitioning into membranes is often better described by Eq. 3 with a constant K than by Eq. 4, and the corresponding fit function for the release experiment based on Eq. 3 is given by:

$$\delta h_i = \left[\gamma\cdot\delta C_L^0\cdot\frac{K\gamma C_D^0}{(1+K\gamma C_L^0)^2} + \gamma\cdot\delta C_D^0\cdot \left(\frac{K\gamma C_L^0}{1+K\gamma C_L^0} - \frac{K\gamma C_L^{syr}}{1+K\gamma C_L^{syr}}\right)\right]\cdot\Delta H_D^{w\to b}\cdot V_{cell} \qquad (15)$$

Here C_D^0 and C_D^{syr} denote the total detergent concentration in the cell and in the syringe, respectively. Note that Eq. 15 is a generalization of Eq. 13 as both C_L^0 and C_D^0 are varied in Eq. 15 whereas only C_L^0 is varied in Eq. 13. For $\delta C_D^0 = 0$ (partitioning experiment), both equations differ only by the factor γ. Fig. 5 shows that all data agree very well with the theoretical curve calculated according to Eq. 15 using $\gamma = 1$.

It should be noted that non-permeating detergents may exhibit a more complex behavior, e.g., if permeation is neither fast ($\gamma = 1$) nor slow ($\gamma = 0.5$) but has an intermediate rate. Furthermore, tensions arising from asymmetric expansion or shrinking of the membrane may also affect $\Delta H_D^{w\to b}$ and K.

3.4. Measurement of the surfactant–membrane partition enthalpy $\Delta H_D^{w\to b}$

A fit of the titration isotherm yields the partition constant K and the partition enthalpy, $\Delta H_D^{w\to b}$. This approach is based on a particular model for the binding process. A model-independent evaluation of $\Delta H_D^{w\to b}$ is possible for detergents with sufficiently large partition constants and experimental conditions such that an almost complete ($>95\%$) binding of detergent to the lipid vesicles can be achieved. Two experimental approaches are possible. The first is a *lipid-into-detergent* titration as shown in Fig. 4 where the final injections yield zero δh_i values. At the end of this titration, almost no detergent has remained free in solution and the molar amount of bound detergent is virtually identical to $n_{D,b} = C_D^0\ V_{cell}$. The cumulative heat is $\sum_{i=1}^{N}\delta h_i$ and the reaction enthalpy is given by

$$\Delta H_D^{w\to b} = \sum_{i=1}^{N}\delta h_i/(C_D^0 V_{cell}) \qquad (16)$$

The second type of experiment is a *detergent-into-lipid* titration, i.e., the reverse experiment as described above. Now the calorimeter cell contains the lipid dispersion and a small amount, δn, of detergent is injected. If the partition constant and the lipid concentration are high enough, practically the total amount of injected detergent is immediately incorporated into the membrane. The reaction enthalpy is thus $\Delta H_D^{w\to b} = \delta h_i/\delta n$ and the partition enthalpy is determined in a *single* injection. Consecutive injections should yield identical results (cf. [18], Fig. 2).

3.5. Other partitioning experiments

The ITC protocol developed by Zhang and Rowe [25,26] is based on the of injection of a lipid/solute mixture of fixed composition into solutions of different solute concentrations. If the free solute concentration in the syringe is lower than the concentration in the cell, further binding to the membrane will occur after injection. If the free solute concentration in the syringe is larger than that in the cell, a solute release will be observed. Binding to or release from the membrane are accompanied by heats of opposite sign. Only if the equilibrium concentration of solute in the syringe matches the solute concentration in the cell, no heat will be measured. Since the solute concentration in the cell is known, one point of the binding isotherm is thus determined and the corresponding partition coefficient K can be calculated. No assumptions regarding the constancy of K and $\Delta H_D^{w\to b}$ must be made and the protocol can be applied also to systems with very low partition coefficients.

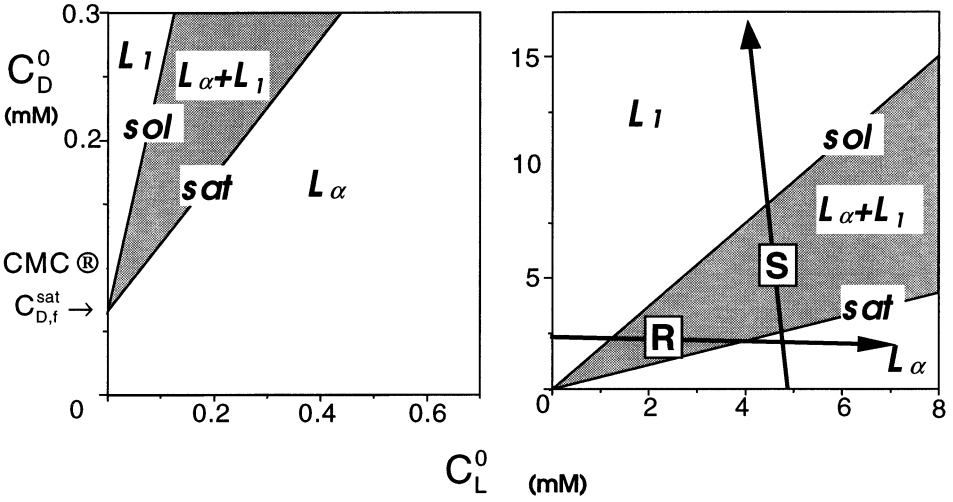

Fig. 6. Schematic phase diagram for lipid–surfactant system at concentrations of the order of the cmc (left panel) or far beyond the cmc (right). The phase boundaries 'sat' and 'sol' separate the lamellar phase (L_α) and the micellar phase (L_1), respectively, from a coexistence range (shaded, $L_\alpha+L_1$). $C_{D,f}^{sat}$ is the minimum concentration of free detergent to induce bilayer disruption. The typical ITC protocols are illustrated as arrows. The membrane solubilization ('S') and membrane reconstitution ('R') protocols should be performed at concentrations far above the cmc (right panel). Then, the phase boundaries can be determined by a single experiment crossing the phase boundaries 'vertically' (solubilization protocol, 'S') or 'horizontally' (reconstitution protocol, 'R'), because the intercept, $C_{D,f}^{sat}$, becomes negligible. The tilt of the arrows from the vertical/horizontal describes the effect of the sample replacement by the titrant.

Another approach has been described by Lichtenberg and coworkers [27]. They injected buffer into lipid/detergent mixtures and detergent was released from the mixed membranes or micelles to establish the equilibrium detergent concentration also in the added volume increment. Assuming that the heat of release, $\Delta H_D^{w\to b} = -\Delta H_D^{w\to b}$ is identical to the heat of demicellization, $\Delta H_D^{m\to w}$, the free detergent concentration can be deduced. However, this assumption must be considered with some caution and is only approximately true. Furthermore, the protocol is restricted to surfactants with a high water solubility (low K) and requires titrations of large volumes, introducing an additional source of errors.

4. Membrane solubilization

Membrane solubilization is usually achieved when the detergent concentration approaches the critical micellar concentration. In the following we discuss

- the *phase diagram*
- the *ITC measuring protocols*

4.1. The surfactant–lipid phase diagram

If a surfactant solution of concentration $C_D^0 > \mathrm{CMC}$ is titrated into a suspension of phospholipid bilayers, the surfactant will initially partition into the membrane forming a mixed lipid–surfactant bilayer. With each injection the concentration of surfactant in the membrane increases until a critical limit C_D^{sat} is reached at which the bilayer will no longer tolerate further detergent and will start to disintegrate. Then, mixed lipid–surfactant bilayers are in equilibrium with lipid–surfactant micelles (bilayer–micelle coexistence range). As the surfactant concentration is increased even further, this equilibrium is shifted towards the micellar structure until a second phase boundary is reached at C_D^{sol} beyond which the bilayer structure can no longer be maintained. At $C_D^0 \geq C_D^{sol}$, mixed lipid–detergent micelles are found in equilibrium with detergent monomers. If the experiment is performed at different lipid concentrations, it is possible to construct a *phase diagram* as shown schematically in Fig. 6 (cf. [12]). The axes in this diagram are the total detergent concentration C_D^0 and the total lipid concentration, C_L^0.

The solid lines are the two phase boundaries, yielding the detergent concentrations C_D^{sat} and C_D^{sol} for a given lipid concentration C_L^0. The titration with surfactant corresponds to a movement parallel to the y-axis in Fig. 6. The phase boundaries C_D^{sat} and C_D^{sol} can easily be detected since discontinuities are observed in some spectroscopic parameters (e.g., turbidity) or the heat of reaction (cf. below) at these characteristic concentrations (cf. [28]).

Experimentally, a linear variation of C_D^{sat} with the total lipid concentration is observed. Since $C_D^0 = C_{D,b} + C_{D,f}$ and $R_b = C_{D,b}/C_L^0$, the detergent concentration at the onset of solubilization, C_D^{sat}, is given by

$$C_D^{sat} = R_b^{sat} \cdot C_L^0 + C_{D,f}^{sat} \quad (17)$$

Eq. 17 predicts that a C_D^{sat} vs. C_L^0 plot intersects the y-axis at $C_{D,f}^{sat}$, i.e., the minimum critical monomer concentration needed to disrupt the bilayer, and has a slope of R_b^{sat}, the limiting ratio of detergent-to-lipid for a stable bilayer. Using Eq. 1 in the form of $R_b^{sat} = K \times C_{D,f}^{sat}$ it is also possible to determine K. A similar equation to Eq. 17 is also valid for the C_D^{sol} curve.

To a first approximation, the coexistence range may be considered a 3-phase range in terms of the Gibbs phase rule. Then, the compositions of each phase were constant and only the total numbers of vesicles and micelles would vary. Hence, the membrane composition remains R_b^{sat}, the surfactant to lipid ratio in the micelles amounts to R_b^{sol} and the monomer concentration is constant so that $C_{D,f}^{sat} = C_{D,f}^{sol}$. Experimental studies have suggested that the monomer concentration increases slightly in the course of solubilization so that $C_{D,f}^{sat} < C_{D,f}^{sol}$ [14,29]. This effect has recently be accounted for by the finite size of the micelles [30] which is in conflict with the phase properties the phase rule is based on.

From an experimental point of view it may be advantageous to start with a detergent solution at concentration C_D^0 and to add successively lipid, i.e., to reverse the order of the experiment described above. This corresponds to a horizontal movement in the phase diagram of Fig. 6. If $C_D^0 \gg C_D^{sol}$, the detergent will initially completely disrupt the added bilayers and mixed lipid–detergent micelles are formed. Next, as the lipid content increases, micelles will be found in coexistence with membranes, and finally, at a sufficiently high lipid concentration, micellar structures will cease to exist and only the bilayer phase remains. The phase boundaries will again be reflected in discontinuities of the experimental parameters.

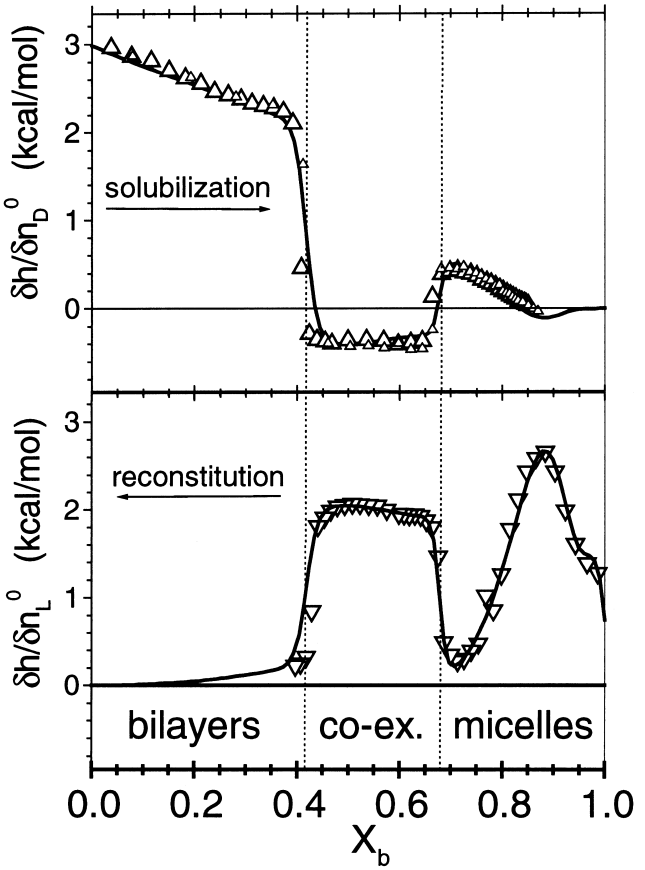

Fig. 7. Titration protocols as exemplified with $C_{12}EO_7$ and POPC vesicles. (A) Titration of 5 mM POPC with 100 mM $C_{12}EO_7$. (B) Titration of 4.9 mM $C_{12}EO_7$ with 15 mM POPC. Data taken from [15].

4.2. The ITC solubilization experiment

The solubilization protocol [7,14,31,32] is based on the injection of detergent at or above the CMC into a vesicle suspension, in order to determine the heat of transfer of a detergent molecule from the micelle to the bilayer, $\Delta H_D^{m \to b}$, and the phase boundaries.

With each injection, δn_D moles of detergent are added to the phospholipid dispersion and the corresponding heat, δh_i, is measured. For a detergent with

a large partition constant K and a sufficiently high lipid concentration an almost complete binding of the added detergent occurs and the *molar* heat, $\delta h_i/\delta n_D$, can be plotted as a function of the mole fraction of detergent in the membrane. This is shown in Fig. 7A for the titration of 100 nm POPC vesicles ($C_L^0 = 5$ mM) with $C_{12}EO_7$ detergent ($C_D^{syr} = 100$ mM) [15]. The lamellar, coexistence and micellar ranges are indicated by endothermic, exothermic, and endothermic heats of titration, respectively, as explained in detail below.

4.2.1. Lamellar range

The equilibrium detergent concentration in the cell during the first few injections remains lower than the critical concentration, $C_{D,f}^{sat}$, needed for membrane solubilization. Hence, the micelles disintegrate into monomers which are incorporated into the lipid membranes. The observed reaction enthalpy, $\Delta H_D^{m\to b}$, is given as the sum of the enthalpy of demicellization, $\Delta H_D^{m\to w} = -\Delta H_D^{w\to m}$, and the partition enthalpy of monomer detergent from water to the bilayer, $\Delta H_D^{w\to b}$:

$$\frac{\delta h_i}{\delta n_D} = \Delta H_D^{m\to b}(X_b) = \Delta H_D^{w\to b}(X_b) - \Delta H_D^{w\to m} \qquad (18)$$

The bilayer partition enthalpy can be dependent on the mole fraction of detergent in the membrane [7,14,15,18]. In the experiment shown in Fig. 7A the reaction enthalpy is initially 3.0 kcal/mol at a very low detergent content in the membrane and decreases linearly to about 2.0 kcal/mol at the onset of bilayer disintegration.

4.2.2. Bilayer–micelle coexistence range

With consecutive injections the free detergent concentration increases until a critical concentration of $C_{D,f}^{sat}$ is reached with a corresponding mole fraction of bound detergent, X_b^{sat}. At this concentration, the mixed lipid-detergent bilayers start to disintegrate and form mixed lipid–detergent micelles. The onset of bilayer solubilization is reflected in a distinct change of the heats of reaction making ITC a sensitive and convenient tool to determine the phase boundaries, X_b^{sat}, and also, X_b^{sol} (cf. below). According to the phase rule approximation (cf. above), the heats of titration, δh_i, are supposed to be constant over the whole coexistence range [7].

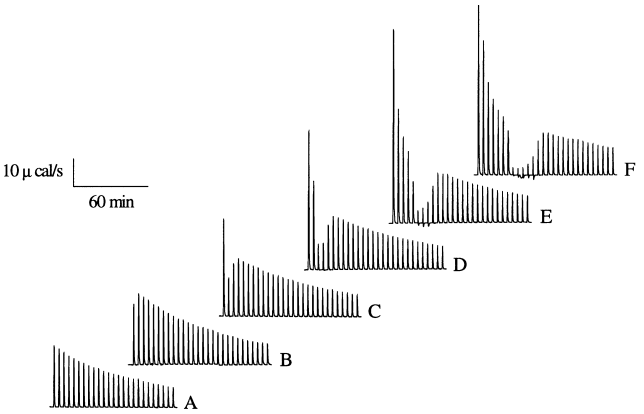

Fig. 8. Titration calorimetry of octyl-β-D-glucopyranoside (C_8Gluc) solutions with sonicated POPC vesicles ($C_L \sim 35$ mM; buffer: 10 mM Tris (pH 7.25), 100 mM NaCl; $T = 28$°C; vesicle diameter ~ 30 nm). Each peak corresponds to the injection of 10 µl of lipid suspension into the reaction cell ($V_{cell} = 1.3353$ ml). The concentration of C_8Gluc in the reaction cell was (A) 15 mM, (B) 16 mM, (C) 17 mM, (D) 18 mM, (E) 20 mM, (F) 22 mM. Upward peaks denote endothermic reactions. From [34].

4.2.3. Micellar range

At detergent concentrations $C_D \geq C_D^{sol}$ (X_b^{sol}) no vesicles are left and only mixed micelles occur in the sample. At this phase boundary, the heat of titration changes again abruptly. Injected detergent micelles equilibrate with lipid–detergent micelles, causing only small heat effects. Under certain conditions, ellipsoidal or rod-like micelles are transformed into spherical micelles upon increasing the detergent content (i.e., decreasing lipid content) [33] giving rise to additional endothermic heats.

4.3. The lipid-into-detergent ITC experiment

The second titration protocol starts with detergent in the calorimeter cell and phospholipid bilayers are successively added. It corresponds to a movement parallel to the x-axis of Fig. 6. The outcome of such a titration is illustrated in Fig. 7B for the titration of $C_{12}EO_7$ with POPC [7] and in more detail in Fig. 8 for octylglucoside [34]. In the latter figure sonicated POPC vesicles are injected into a solution of octylglucoside (cf. also [14,27]). The simplest situation is encountered when the detergent concentration is distinctly below the CMC of C_8Gluc (CMC $\approx$ 22.6 mM at 30°C, [6,35]) as shown in 8A. Each injection leads to incorporation of surfactant

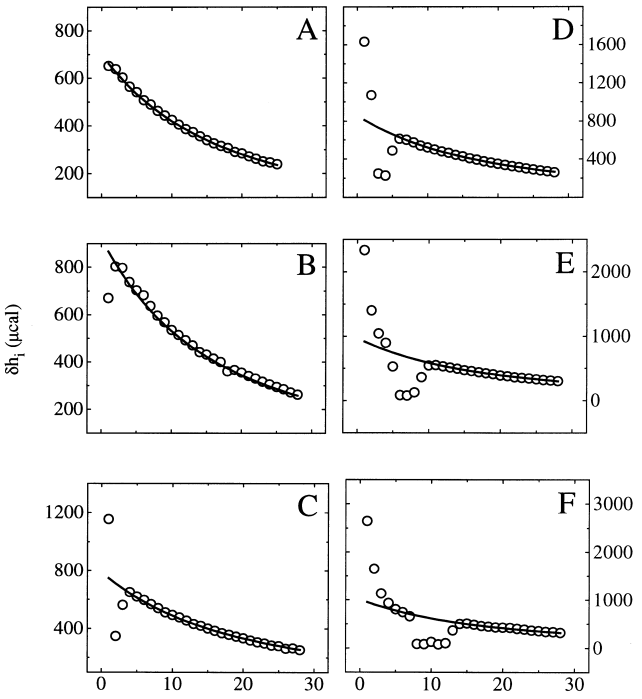

Fig. 9. Comparison between experimental titration curves and theoretical predictions based on the partition model $X_b = K C_{D,f}$. The open circles are the experimental titration peaks $\delta h_i = h_i - h_{d,i}$ as measured in Fig. 8 (h_i) and corrected for dilution effects ($h_{d,i}$). The solid lines are calculated with the partition model (Eq. 3): (A) C_8Gluc concentration $C_D^0 = 15$ mM, simulation parameter $K = 90$ M^{-1}, $\Delta H_D^0 = 1.7$ kcal/mol; (B) $C_D^0 = 16$ mM, $K = 90$ M^{-1}, $\Delta H_D^{w\to b} = 1.75$ kcal/mol; (C) $C_D^0 = 17$ mM, $K = 84$ M^{-1}, $\Delta H_D^{w\to b} = 1.77$ kcal/mol; (D) $C_D^0 = 18$ mM, $K = 90$ M^{-1}, $\Delta H_D^{w\to b} = 1.695$ kcal/mol; (E) $C_D^0 = 20$ mM, $K = 88$ M^{-1}, $\Delta H_D^{w\to b} = 1.71$ kcal/mol; (F) $C_D^0 = 22$ mM, $K = 85$ M^{-1}, $\Delta H_D^{w\to b} = 1.67$ kcal/mol. From [34].

and produces an endothermic heat of reaction which decreases smoothly with consecutive injections. With each lipid injection the concentration of free detergent is reduced, less detergent is available for binding, and the experimental heat of reaction decreases. This experiment is quantitatively described by the partition equilibrium (Eqs. 3 and 13).

At higher surfactant concentrations ($C_D^0 > 16$ mM) a more complicated titration pattern appears which can be formally divided into three distinct regions. For the first N injections, the endothermic heat of reaction decreases monotonously. At step N+1, the reaction enthalpy shows a discontinuity. This second phase of the titration experiment comprises again about N injection steps. The reaction enthalpy drops close to zero and a fast endothermic and a slower exothermic reaction can be discerned. The endothermic enthalpy then increases in magnitude and dominates the reaction toward the end of phase II. The third phase is characterized by a smooth decrease in the reaction enthalpy.

The explanation of this complex titration pattern is given in Fig. 9. The basic process is C_8Gluc partitioning into the membrane which is endothermic with $\Delta H_D^{w\to b} = 1.75$ kcal/mol and described by the partition equilibrium (solid line in Fig. 9). The deviations from the theoretical line arise from *membrane disintegration* and *membrane formation*. During the first N injections, the endothermic heat due to detergent partitioning is *enhanced* by a second endothermic process which must be ascribed to a transformation of mixed lipid–detergent bilayers into mixed micelles. If the detergent concentration in the cell is close to or above the CMC, C_8Gluc partitioning is followed by *membrane disintegration* and mixed C_8Gluc/POPC micelles are in equilibrium with C_8Gluc monomers. This process is characterized by an endothermic micellization enthalpy of $\Delta H \approx +1.85$ kcal/mol. After N injections the process of micelle formation comes to a halt. The concentration of free detergent is no longer large enough to disrupt the bilayers. In fact, addition of further lipid will reverse the process of micelle formation. The concentration of mixed lipid–detergent micelles will decrease in favor of the *formation of mixed bilayers* and the enthalpy consumed in bilayer→micelle transition will be returned. The exothermic enthalpy of bilayer reconstitution, $\Delta H = -1.85$ kcal/mol, is superimposed on the endothermic partitioning. The third phase of the titration experiment then corresponds to a pure partitioning since no mixed micelles exist after about $2N$ injection steps.

The partition coefficient of octylglucoside (C_8Gluc) is $K = 120$ M^{-1} and a considerable fraction of the detergent is present as monomers during the whole titration experiment. In contrast, the partition coefficient of $C_{12}EO_7$ is $K = 12 \times 10^3$ M^{-1} and the detergent monomer concentration is negligible. Under conditions of strong detergent binding it can be useful to normalize the heats of reaction, δh_i, by the molar amount of injected detergent δn_D as shown for the $C_{12}EO_7$–POPC system in the middle panel of Fig. 7. Again the normalized heat of reaction is plotted as a function of the mole fraction of detergent in

the lipid-detergent system. The titration starts at $X_D = 1$ (only $C_{12}EO_7$ is in the calorimeter cell). As the injected phospholipid vesicles are converted into mixed micelles, ΔH_D varies considerably until the bilayer-micelle coexistence phase is reached where ΔH_D remains constant over the whole coexistence range.

5. Thermodynamic parameters of surfactant–membrane partitioning

Thermodynamic data for the partitioning of non-ionic surfactants into POPC membrane vesicles are summarized in Table 1. Most ITC results were obtained with ~100 nm vesicles (prepared by extrusion through polycarbonate filters). For octylglucoside comparative measurements were made with 30 nm vesicles (prepared by ultrasound sonication) [21]. No difference in $\Delta H_D^{w\to b}$ and K were found for the two types of vesicles. (This is distinctly different from ITC studies with peptides and proteins where strongly exothermic reaction enthalpies are measured for 30 nm vesicles but much less exothermic or even endothermic $\Delta H_D^{w\to b}$ values for 100 nm vesicles [36–38]).

All partition enthalpies are *endothermic* and are of the order of $\Delta H_D^{w\to b} \sim 2$–4 kcal/mol. Table 1 reveals a weak dependence of $\Delta H_D^{w\to b}$ on the *length* of the hydrocarbon chain. The surfactants with shorter hydrocarbon chain have the more endothermic $\Delta H_D^{w\to b}$ for a given headgroup. A better documented correlation is seen between the partition enthalpy and the *size of the headgroup*. The comparison of the surfactants $C_{12}EO_n$ with $n = 3...8$ shows an increase in $\Delta H_D^{w\to b}$ by about 1 kcal/mol per ethylene oxide unit. Likewise, the change from the glucose headgroup to the larger and more polar maltose headgroup increases $\Delta H_D^{w\to b}$ by 1–2 kcal/mol.

The temperature dependence of the partition enthalpy has been measured for octylglucoside (C_8 Gluc) [21], octylthioglucoside (C_8 TGluc) [18,21], and $C_{12}EO_8$ [32]. The partition enthalpy decreases with increasing temperature and changes its sign typically somewhat above room temperature. The specific heat capacity for the transfer from water into the lipid membrane is negative with $\Delta C_p = -75$ cal/(mol·K) for C_8 Gluc, −98 cal/(mol·K) for C_8 TGluc, and −220 to −170 cal/(mol·K) for $C_{12}EO_8$ (dependent on concentration).

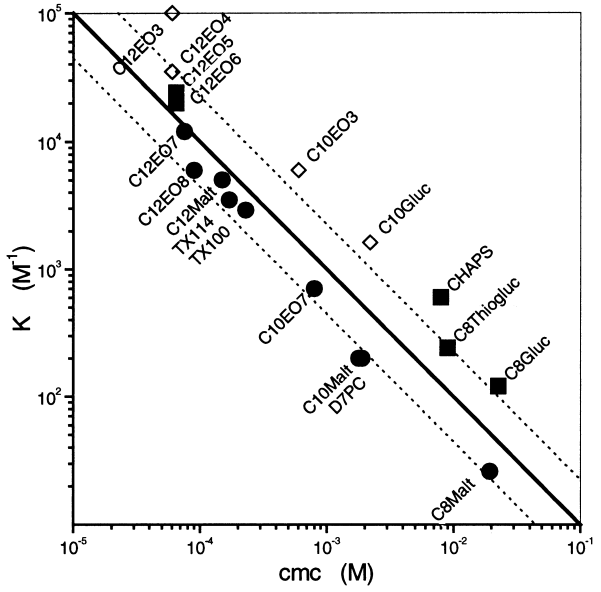

Fig. 10. Membrane partitioning and micelle formation. Double logarithmic plot of the partition constant K vs. the critical micellar concentration CMC. The solid line represents the relationship $K \cdot CMC = 1$. The lower dashed line summarizes the 'strong' detergents with $R_b^{sat} \sim 0.6$, the upper dashed line the 'weak' detergents which can be incorporated into the membrane up to detergent-to-lipid ratios of $R_b \sim 1.4$–1.6. From [22].

Reaction enthalpies close to zero and large negative heat capacities are typical for the transfer of hydrophobic molecules from the aqueous phase into an organic environment. For example, the transfer of hexane from water to the organic phase is characterized by $\Delta H^0 \approx 0$ kcal/mol (at 25°C) and $\Delta C_p = -105$ cal/(mol·K) [39]. The partitioning of a surfactant into a lipid membrane is hence an entropy-driven reaction and constitutes a classical example of the so-called hydrophobic effect. In this model, the surfactant in the aqueous phase is surrounded by structured water which is released as soon as the surfactant enters the membrane. The change in the dynamics of water adjacent to hydrophobic surfaces is thought to be responsible for the large negative heat capacity.

Micelle formation and partitioning into the lipid membrane are two energetically closely related processes. In order to minimize unfavorable interactions with water, a detergent molecule can either associate with other monomers to form a micelle or intercalate

between lipid molecules. The standard free energy of micellization is

$$\Delta G_D^{0,w\to m} = +RT\ln(CMC/55.5) \quad (19)$$

that of bilayer partitioning

$$\Delta G_D^{0,w\to b} = -RT\ln(55.5K) \quad (20)$$

The factor 55.5 corresponds to the molar concentration of water (cf. above) and accounts for the fact that the concentration of detergent in solution should be given by its mole fraction rather than by mol/l [10,40]. At $K{\cdot}CMC = 1$ both processes have equal standard free energies.

Micellization, partitioning into membranes, and formation of mixed lipid/surfactant micelles are thus expected to be intimately connected [11]. Fig. 10 shows a double logarithmic plot of K vs. CMC (taken from [22]). The solid line in the diagram has a slope of -1 and corresponds to $K{\cdot}CMC = 1$. The figure shows that a linear relationship can be established between the two parameters. In fact, strong and weak detergents can be distinguished [22]. 'Strong' detergents are defined by $K{\cdot}CMC < 1$, 'weak' detergents by $K{\cdot}CMC > 1$. The two groups are represented by the lower and upper dashed lines of Fig. 10, which correspond to deviations of ± 2 kJ/mol (± 0.48 kcal/mol) in standard free energy. For strong detergents the average value $\langle K{\cdot}CMC\rangle \approx 0.6$ and the detergent-to-lipid ratio at which the membranes disintegrate is also about the same value. i.e., $R_b^{sat} \sim 0.6$. For weak detergents $K{\cdot}CMC \sim 1.8 \pm 0.7$ and the saturation limit is $R_b^{sat} \sim 1.76 \pm 0.7$. For a given length of the hydrocarbon chain 'strong' detergents have a larger (and more polar) headgroup than 'weak' detergents. The relationship

$$K \sim \frac{1}{CMC} \quad (21)$$

allows a rough estimate (within one order of magnitude) of the membrane partition constant from the critical micellar concentration and vice versa.

Future applications of isothermal titration calorimetry may involve the quantitative analysis of *domain formation* in biological membranes. A variety of studies suggests that biomembranes contain in parallel domains with lipids in the liquid-ordered state (L_0) and others in the more fluid, liquid-crystalline state (L_α). The L_0 domain appears to be rich in cholesterol and saturated lipids, the L_α domain collects preferentially unsaturated phospholipids [41,42]. Operationally, the two domains can be differentiated by their behavior towards Triton X-100 at 4°C. L_0 domains are insoluble in Triton X-100 (detergent resistant membranes), whereas L_α domains are apparently soluble in this detergent. The quantitative information on domain formation are scarce; likewise the reason for Triton X-100 insolubility is also not well-understood. Since lipid domains (lipid 'rafts') are considered to be functional units, regulating the membrane properties, a quantitative understanding of the parameters leading to domain formation is of biological importance. Isothermal titration calorimetry could be a convenient tool to provide such thermodynamic information.

Acknowledgements

We are indebted to G. Fedrigo for measurements with the CHAPS detergent. This work was supported by the Swiss National Science Foundation Grant no. 31-42058.94.

Abbreviations

δh_i	absolute heat of the ith injection
γ	asymmetry parameter
C	molar concentration
$C_{12}EO_8$	octa(ethylene glycol) dodecyl ether
C_8-Gluc	*n*-octyl-β-D-glucopyranoside
C_8-TGluc	*n*-octyl-β-D-thioglucopyranoside
CFB	power of the cell heater (adjustable)
CMC	critical micelle concentration
i	injection index
ITC	isothermal titration calorimetry
JFB	power of the jacket heater (adjustable)
K	mole ratio partition coefficient
n	mole number
P	mole fraction partition coefficient
POPC	1-palmitoyl-2-oleoyl-*sn*-glycero-3-phosphocholine
R	gas constant, 8.314 J/(mol K)
R_b	mole ratio of surfactant per lipid in the membrane
RO	power of the reference cell heater (constant)
rpm	rounds per minute
T	temperature

V	volume
X_b	mole fraction of surfactant within a membrane
ΔG^0	difference in molar standard free energy
ΔH	difference in molar enthalpy
ΔS	difference in molar entropy
ρ^0	non-ideality parameter
Indices and superscripts	
b	bound to the membrane
cell	referring to the cell
D	of the detergent
f	free in solution
inj	referring to the injection
L	of the lipid
sat	at membrane saturation (the onset of solubilization)
sol	at the completion of solubilization
syr	in the injection syringe
0	total (except ΔG^0)
W	of water
$w \rightarrow b$	upon transfer from water into bilayer
$w \rightarrow m$	upon transfer from water into micelle
$m \rightarrow b$	upon transfer from micelle into bilayer

References

[1] T. Wiseman, S. Williston, J.F. Brandts, L.-N. Lin, Rapid measurement of binding constants and heats of binding using a new titration calorimeter, Anal. Biochem. 179 (1989) 131–137.

[2] G.C. Kresheck, W.A. Hargraves, Thermometric titration studies of the effect of head group, chain length, solvent, and temperature on the thermodynamics of micelle formation, J. Colloid Interface Sci. 48 (1974) 481–493.

[3] G.C. Kresheck, Comparison of the calorimetric and van't Hoff enthalpy of micelle formation for a nonionic surfactant in H_2O and D_2O solutions from 15 to 40°C, J. Phys. Chem. B 102 (1998) 6596–6600.

[4] G. Olofsson, Microtitration calorimetric study of the micellization of three poly (oxyethylene) glycol dodecyl ethers, J. Phys. Chem. 89 (1985) 1473.

[5] I. Johnson, G. Olofsson, B. Jönsson, Micelle formation of ionic amphipiles, J. Chem. Soc. Faraday Trans. 183 (1987) 3331–3344.

[6] S. Paula, W. Süs, J. Tuchtenhagen, A. Blume, Thermodynamics of micelle formation as a function of temperature: A high sensitivity titration calorimetry study, J. Phys. Chem. 99 (1995) 11742–11751.

[7] H. Heerklotz, G. Lantzsch, H. Binder, G. Klose, A. Blume, Thermodynamic characterization of dilute aqueous lipid/detergent mixtures of POPC and C12EO8 by means of isothermal titration calorimetry, J. Phys. Chem. 100 (1996) 6764–6774.

[8] H. Heerklotz, R.M. Epand, The enthalpy of acyl chain packing and the apparent water accessible apolar surface area of phospholipids, Biophys. J. (2000) in press.

[9] P. Schurtenberger, N. Mazer, W. Kanzig, Micelle to vesicle transition in aqueous-solutions of bile-salt and lecithin, J. Phys. Chem. 89 (1985) 1042–1049.

[10] C. Tanford, The Hydrophobic Effect: Formation of Micelles and Biological Membranes, 2nd. ed., Wiley, New York, 1980.

[11] D. Lichtenberg, Characterization of the solubilization of lipid bilayers by surfactants, Biochim. Biophys. Acta 821 (1985) 470–478.

[12] D. Lichtenberg, in: M. Shinitzky (Ed.), Biomembranes – Physical Aspects VCH, Weinheim, 1993, pp. 63–96.

[13] M. Ueno, Partition behavior of a nonionic detergent, octyl glucoside, between membrane and water phases, and its effect on membrane permeability, Biochemistry 28 (1989) 5631–5634.

[14] M. Keller, A. Kerth, A. Blume, Thermodynamics of interaction of octyl glucoside with phosphatidylcholine vesicles: partitioning and solubilization as studied by high sensitivity titration calorimetry, Biochim. Biophys. Acta 1326 (1997) 178–192.

[15] H.H. Heerklotz, H. Binder, H. Schmiedel, Excess enthalpies of mixing in phospholipid-additive membranes, J. Phys. Chem. B 102 (1998) 5363–5368.

[16] H. Heerklotz, H. Binder, G. Lantzsch, G. Klose, Membrane/water partition of oligo(ethylene oxide) dodecyl ethers and its relevance for solubilization, Biochim. Biophys. Acta 1196 (1994) 114–122.

[17] J. Lasch, Interaction of detergents with lipid vesicles, Biochim. Biophys. Acta 1241 (1995) 269–292.

[18] M.R. Wenk, J. Seelig, Interaction of octyl-β-thioglucopyranoside with lipid membranes, Biophys. J. 73 (1997) 2565–2574.

[19] J. Seelig, P. Ganz, Non-classical hydrophobic effect in membrane binding equilibria, Biochemistry 30 (1991) 9354–9359.

[20] J. Seelig, Titration calorimetry of lipid-peptide interactions, Biochim. Biophys. Acta 1331 (1997) 103–116.

[21] M.R. Wenk, T. Alt, A. Seelig, J. Seelig, Octyl-β-D-glucopyranoside partitioning into lipid bilayers: thermodynamics of binding and structural changes of the bilayer, Biophys. J. 72 (1997) 1719–1731.

[22] H. Heerklotz, J. Seelig, Correlation of membrane/water partition coefficients of detergents with the critical micelle concentration, Biophys. J. 78 (2000) 2435–2440.

[23] U. Kragh-Hansen, M. le Maire, J.V. Moller, The mechanism of detergent solubilization of liposomes and protein-containing membranes, Biophys. J. 75 (1998) 2932–2946.

[24] H.H. Heerklotz, H. Binder, R.M. Epand, A 'release' protocol for isothermal titration calorimetry, Biophys. J. 76 (1999) 2606–2613.

[25] F. Zhang, E.S. Rowe, Titration calorimetric and differential scanning calorimetric studies of the interactions of n-butanol with several phases of dipalmitoylphosphatidylcholine, Biochemistry 31 (1992) 2005–2511.

[26] F. Zhang, E.S. Rowe, Calorimetric studies of the interac-

tions of cytochrome c with dioleoylphosphatidylglycerol extruded vesicles: ionic strength effects, Biochim. Biophys. Acta 1193 (1994) 219–225.
[27] E. Opatowski, D. Lichtenberg, M.M. Kozlov, The heat of transfer of lipid and surfactant from vesicles into micelles in mixtures of phospholipid and surfactant, Biophys. J. 73 (1997) 1458–1467.
[28] S. Almog, B.J. Litman, W. Wimley, J. Cohen, E.J. Wachtel, Y. Barenholz, A. Ben-Shaul, D. Lichtenberg, States of aggregation and phase transformations in mixtures of phosphatidylcholine and octyl glucoside, Biochemistry 29 (1990) 4582–4592.
[29] E. Opatowski, M.M. Kozlov, D. Lichtenberg, Partitioning of octyl glucoside between octyl glucoside/phosphatidylcholine mixed aggregates and aqueous media as studied by isothermal titration calorimetry, Biophys. J. 73 (1997) 1448–1457.
[30] Y. Roth, E. Opatowski, D. Lichtenberg, M.M. Kozlov, Phase behavior of dilute aqueous solutions of lipid–surfactant mixtures: Effects of finite size of micelles, Langmuir 26 (2000) 2052–2061.
[31] H. Heerklotz, G. Lantzsch, H. Binder, G. Klose, A. Blume, Application of isothermal titration calorimetry for detecting lipid membrane solubilization, Chem. Phys. Lett. 235 (1995) 517–520.
[32] H. Heerklotz, H. Binder, G. Lantzsch, G. Klose, A. Blume, Lipid/detergent interaction thermodynamics as a function of molecular shape, J. Phys. Chem. B 101 (1997) 639–645.
[33] T. Gutberlet, M. Kiselev, H. Heerklotz, G. Klose, SANS study of mixed POPC/$C_{12}E_n$ aggregates, Physica B 276-278 (2000) 381–383.
[34] M.R. Wenk, J. Seelig, Vesicle-micelle transformation of phosphatidylcholine/octyl-β-D-glucopyranoside mixtures as detected with titration calorimetry, J. Phys. Chem. B 101 (1997) 5224–5231.
[35] M.L. Antonelli, M.G. Bonicelli, G. Ceccaroni, C. La Mesa, B. Sesta, Solution properties of octyl-beta-D-glucoside. 2. Thermodynamics of micelle formation, Colloid Polymer Sci. 272 (1994) 704.
[36] G. Beschiaschvili, J. Seelig, Peptide binding to lipid bilayers. Nonclassical hydrophobic effect and membrane-induced pK shifts, Biochemistry 31 (1992) 10044–10053.
[37] J.A. Gazzara, M.C. Phillips, S. Lund-Katz, M.N. Palgunachari, J.P. Segrest, G.M. Anantharamaiah, W.V. Rodriguez, J.W. Snow, Effect of vesicle size on their interaction with class A amphipathic helical peptides, J. Lipid Res. 38 (1997) 2147–2154.
[38] M.R. Wenk, J. Seelig, Magainin 2 amide interaction with lipid membranes: calorimetric detection of peptide binding and pore formation, Biochemistry 37 (1998) 3909–3916.
[39] P.L. Privalov, S.J. Gill, Stability of protein structure and hydrophobic interaction, Adv. Protein. Chem. 39 (1988) 191–234.
[40] C.R. Cantor, P.R. Schimmel, Biophysical Chemistry, vol. 1, Freeman, San Francisco, 1980.
[41] D.A. Brown, E. London, Structure and origin of ordered lipid domains in biological membranes, J. Membr. Biol. 164 (1998) 103–114.
[42] A. Rietveld, K. Simons, The differential miscibility of lipids as the basis for the formation of functional membrane rafts, Biochim. Biophys. Acta 1376 (1998) 467–479.
[43] Sigma Catalogue
[44] S. Saito, T. Tsuchiya, Characteristics of *n*-octyl beta-D-thioglucopyranoside, a new non-ionic detergent useful for membrane biochemistry, Biochem. J. 222 (1984) 829–832.
[45] J.C. Brackman, N.M. Vanos, J. Engberts, Polymer nonionic micelle complexation – formation of poly(propylene oxide)-complexed *n*-octyl thioglucoside micelles, Langmuir 4 (1988) 1266–1269.
[46] Anatrace Catalogue